frontiers in Marine Science

ORIGINAL RESEARCH
published: 02 July 2019
doi: 10.3389/fmars.2019.00357

Theoretical Assessment of the Effect of Vertical Dispersivity on Coastal Seawater Radium Distribution

Sébastien Lamontagne[1] and Ian T. Webster[2]*

[1] CSIRO Land & Water, Waite Laboratories, Urrbrae, SA, Australia, [2] Retired, Canberra, ACT, Australia

Trends in radium (Ra) activity in coastal seawater are frequently used to infer submarine groundwater discharge. In general, unlike in the deep oceans, Ra samples are only collected from the surface of the mixed layer in coastal areas. The assumption is that the water column is well mixed, as often evidenced by uniform temperature and salinity profiles. However, if the timescale for vertical mixing is similar to or less than the timescale for radioactive decay, the vertical profiles in Ra activity may not be uniform. In the present work, a two-dimensional dispersion model was developed to evaluate the potential effects of slow vertical mixing on Ra distribution in the mixed layer of an inner shelf. The variables considered were the vertical coefficient of solute dispersivity (K_z), the offshore coefficient of solute dispersivity (K_x), the coastal Ra flux (F_o), the benthic Ra flux (F_B), and the slope of the seabed. The shorter-lived Ra isotopes (^{223}Ra and ^{224}Ra; $t_{1/2}$ = 3.66 and 11.4 days, respectively) were sensitive to K_z when its value was low ($<10^{-4}$ m^2 s^{-1}), resulting in complex activity patterns in the water column as a function of the other variables. Ra-228 ($t_{1/2}$ = 5.75 years) was only moderately impacted by low K_z but the long-lived ^{226}Ra ($t_{1/2}$ = 1600 years) was insensitive to K_z. Surface water samples may not always be representative of water column Ra activity when K_z is low, which will need to be taken into account in future field programs for seawater Ra distribution in shelf environments.

Keywords: submarine groundwater discharge, radium, dispersion, vertical mixing, seawater

OPEN ACCESS

Edited by:
Henrietta Dulai, University of Hawai'i at Mānoa, United States

Reviewed by:
Joseph James Tamborski, Woods Hole Oceanographic Institution, United States
Jennifer Joan Verduin, Murdoch University, Australia

****Correspondence:***
Sébastien Lamontagne
sebastien.lamontagne@csiro.au

Specialty section:
This article was submitted to Marine Ecosystem Ecology, a section of the journal Frontiers in Marine Science

Received: *01 March 2019*
Accepted: *07 June 2019*
Published: *02 July 2019*

Citation:
Lamontagne S and Webster IT (2019) Theoretical Assessment of the Effect of Vertical Dispersivity on Coastal Seawater Radium Distribution. Front. Mar. Sci. 6:357. doi: 10.3389/fmars.2019.00357

INTRODUCTION

The radium (Ra) quartet (^{223}Ra, ^{224}Ra, ^{226}Ra, and ^{228}Ra) are among the most commonly used environmental tracers for evaluating submarine groundwater discharge (SGD) (Charette and Scholten, 2008), including its terrestrial groundwater and recirculated seawater components (Burnett et al., 2003). One common experimental design to evaluate SGD with these tracers is to collect water samples along transects perpendicular to the shoreline, and use simple advective-dispersive transport models to quantify the offshore coefficient of solute dispersivity (K_x), the tracer flux from the coastline (F_o), and the tracer flux from the seabed (F_B) (Moore, 2000; Hancock et al., 2006). Several assessments have been made of the validity of this approach. For example, Knee et al. (2011) have shown how activity measurement error can bias the application of the Ra transport models, Moore (2015) highlighted some of the limitations in the use of ^{228}Ra and ^{226}Ra to evaluate mixing and advection rates, Li and Cai (2011) evaluated the effect of neglecting advection on K_x estimates, and Lamontagne and Webster (2019) showed how K_x could be tracer-dependent.

However, unlike in deep oceans and shelf environments, where ^{228}Ra, ^{226}Ra, and ^{222}Rn vertical profiles have been used to estimate vertical mixing (Broecker et al., 1967; Chung and Craig, 1973; Glover and Reeburgh, 1987; Koch-Larrouy et al., 2015), Ra measurement in shallower inner shelf environments are typically only taken from the top of the mixed layer (Moore, 2000; Dulaiova and Burnett, 2006; Lamontagne et al., 2008). The assumption is that vertical mixing is relatively rapid in the mixed layer so Ra activities should be approximately uniform vertically. However, few studies have been conducted to test this assumption (see below). A water column may appear to be well mixed as evidenced by near uniformity in temperature or salinity profiles but may appear to be less well mixed for radioactive tracers if the timescale of mixing is similar to, or longer, than the timescale of radioactive decay.

Where vertical Ra profiles have been measured on the inner shelf, some variations in activity have been reported. For example, Moore et al. (1995) observed noticeable vertical variations in ^{226}Ra, ^{228}Ra, and ^{224}Ra on the Amazon shelf, but these were attributed in part to variations in salinity (i.e., mixing of different sources of water). Levy and Moore (1985) observed increases in ^{224}Ra activity with depth in the mixed layer off the coast of South Carolina and Georgia, which they attributed to input from the seafloor. During an extensive survey of the South Atlantic Bight, occasional sampling near the surface and the bottom of the mixed layer showed that in most cases Ra activities were similar (Moore, 2007). Thus, vertical variations in Ra activity in the mixed layer may occur under some conditions in inner shelf environments.

Here, a theoretical assessment was made to show how variations in the vertical mixing rate could influence water column Ra activities in a shelf environment. As the focus here was on the short-lived Ra isotopes (^{223}Ra and ^{224}Ra), only dispersive transport was considered because advective transport in the offshore direction is usually not important for them (Lamontagne and Webster, 2019). The assessment was made by developing a two-dimensional model that included dispersion in the vertical direction, based on a previous one-dimensional offshore dispersive transport model by Hancock et al. (2006). In a first step, the effect of variations in the vertical coefficient of solute dispersivity (K_z) on Ra distribution in the water column was evaluated. In a second step, the effect of other transport variables (K_x, F_o, and F_B) on Ra distribution in the water column was evaluated.

In the following, the 2D model is described along with the range in parameter values considered. Whether the current experimental design for tracer surveys in coastal areas provides biased estimates of water column Ra activities is discussed.

MATERIALS AND METHODS

In this study, the model domain for Ra transport was considered to be the cross-section of a sloping continental shelf (**Figure 1**). The sources of Ra to the water column were from the coast and the seabed. Tracer transport was assumed to occur via dispersive processes only, which can be described by the diffusion equation in the x (offshore) and z (depth) directions:

$$\frac{\partial A}{\partial t} = \frac{\partial K_x \partial A}{\partial^2 x} + \frac{\partial K_z \partial A}{\partial^2 z} - \lambda A \quad (1)$$

where A is the Ra activity, t is time and λ the decay constant for a given isotope. Considering the steady-state condition and anisotropic cross-section, Eq. (1) simplifies to:

$$K_x \frac{\partial^2 A}{\partial x^2} + K_z \frac{\partial^2 A}{\partial z^2} = \lambda A \quad (2)$$

This equation was solved numerically using the finite difference method. The numerical grid incorporated a single cell at the coastline and 200 vertical cells at the offshore boundary (**Figure 1**). Boundary conditions included a constant flux F_o (Bq m^{-1} s^{-1}) at the coastline and a constant benthic flux F_B (Bq m^{-1} s^{-1}) spread evenly between the cells on the seabed. A no-flux boundary condition (F_e = 0) was assigned to the offshore end. Cell dimensions were 200 m in the x and 2 m in the z directions, ensuring the offshore boundary was far enough away from the coast (40 km) in order to reasonably meet the F_e = 0 boundary condition at this boundary (vertical profiles were investigated for the first 10 km only).

The literature was scanned for a reasonable range in K_x, K_z, F_o, and F_B for a shelf environment – these are summarized in **Tables 1**, **2**. In a first step, Eq. (2) was solved for different K_z values for each Ra isotope using default values for K_x, F_o, and F_B (**Table 2**). This process identified which isotope if any was sensitive to variations in K_z in terms of uneven activity distribution in the water column. For those isotopes sensitive to K_z, the additional effects of variations in K_x, F_o, F_B, and seabed slope (m) on vertical Ra distribution were evaluated for a relatively low K_z value. The MATLAB script used to solve Eq. (2) is provided as **Supplementary Material**.

RESULTS

K_z

The range of K_z values found in the literature – including both coastal and deep ocean areas – spanned 7.5 × 10^{-6} to 10^{-1} m^2 s^{-1}. Thus, K_z values ranging from 10^{-6} to 10^{-2} m^2 s^{-1} were used here. Variations in K_z did result in noticeable changes in the vertical and horizontal distribution of the shorter-lived tracers. For example, when using the default values for F_o and F_B for ^{223}Ra, K_z = 10^{-6} m^2 s^{-1}, and K_x = 10 m^2 s^{-1}, ^{223}Ra distribution was clearly lower at the surface than at depth at a given distance from the shoreline, especially when farther offshore (**Figure 2**).

The simulations showed that vertical patterns in Ra activity as a function of K_z were complex, with the highest activities either at the surface, the seabed, or at intermediate depths depending on the magnitude of K_z, the Ra isotope, and the offshore distance. To emphasize these, vertical variations in Ra activity were demonstrated at x = 2, 5, and 10 km for various K_z values (**Figure 3**). In general, water column Ra activity was nearly constant when K_z > 10^{-4} m^2 s^{-1}, with the exception of the longest – lived ^{226}Ra which was insensitive to K_z under

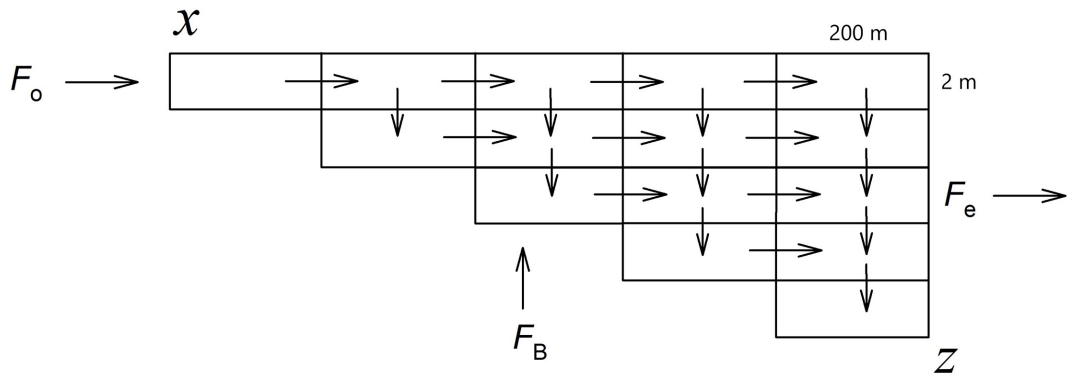

FIGURE 1 | Conceptual representation of the cross-section for a sloping continental shelf with key boundary conditions controlling the Ra flux. F_o, coastal flux; F_B, benthic flux; F_e, offshore boundary flux (set to 0). Solute exchange between cells occurs via dispersive processes.

the conditions tested. For the cases when $K_z < 10^{-4}$ m^2 s^{-1}, ^{223}Ra and ^{224}Ra activities were highest near the seabed at 2 km and in proximity of the surface at 5 and 10 km. The differences in activity through the water column were substantial at low K_z values for ^{223}Ra and ^{224}Ra. For example, ^{224}Ra activities at 2 km were ∼2 mBq L^{-1} near the surface and ∼ 5 mBq L^{-1} near the seabed. The differences in activity through the water column were more subdued for ^{228}Ra and only noticeable at the lowest K_z value. For example, ^{228}Ra at 2 km varied from ∼0.30 to ∼0.35 mBq L^{-1} through the water column (which would probably not be apparent in a field setting due to measurement uncertainty). Overall, only sampling for surface water would tend to bias the estimate of water column activity at low K_z values for ^{223}Ra, ^{224}Ra, and possibly ^{228}Ra but not for ^{226}Ra under the conditions evaluated.

K_x

In addition to slow mixing of the water column, the complex distribution in Ra activity at low K_z also reflects the presence of two sources of Ra (coast and seabed) and how Ra from these sources is being dispersed through the water mass, especially as it becomes deeper offshore. Firstly, the effect of K_x was evaluated for ^{224}Ra, ^{223}Ra, and ^{228}Ra for a relatively low K_z value (10^{-5} m^2 s^{-1}). Ra-226 was not evaluated because it was insensitive to K_z under the conditions tested, as demonstrated in the previous section.

The horizontal and vertical ^{223}Ra and ^{224}Ra distributions were substantially impacted by variations in K_x (**Figure 4**). In general, there was a tendency for the lowest ^{223}Ra and ^{224}Ra activities to be found near the seabed at low K_x values and near the surface at the higher K_x values. For example, for ^{224}Ra at 5 km (**Figure 4B**), activities were ∼0.5 mBq L^{-1} near the surface and ∼0.1 mBq L^{-1} near the seabed for $K_x \leq 1$ m^2 s^{-1} but ∼0.3 mBq L^{-1} near the surface and ∼1.5 mBq L^{-1} near the seabed for $K_x = 100$ m^2 s^{-1}. In other words, with a low K_z and a high K_x, there is a tendency for Ra produced via a benthic source to be exported in the offshore direction rather than to be mixed into the overlying water column (see also **Figure 2**). Whilst the overall magnitude of the activity changed, unlike for ^{223}Ra and ^{224}Ra, variations in K_x did not noticeably change the vertical distribution in ^{228}Ra.

F_o, F_B, and Seabed Slope

For simplicity, this part of the analysis only considered ^{224}Ra (the worst-case scenario due to its shortest half-life). Variations in the magnitude of the coastal and seabed fluxes as well as seabed slope had a noticeable impact on the vertical ^{224}Ra profiles (using $K_z = 10^{-5}$ m^2 s^{-1}). Changing the magnitude of F_o changed vertical ^{224}Ra profiles when getting closer to the shoreline (**Figures 5A,B**) but not offshore (**Figure 5C**). This demonstrated that the coastal flux does not contribute any ^{224}Ra to the water column at 10 km and beyond under the conditions tested (i.e., all the ^{224}Ra originates from the seabed). In contrast, variations in F_B impacted the profiles at 2, 5, and 10 km with a tendency for ^{224}Ra activity to be highest near the surface at higher F_B (**Figures 5D–F**) This may seem counterintuitive at first but can be explained by the sloping seabed. The highest ^{224}Ra activities occur near the shoreline due the combined F_o and F_B fluxes and a smaller dilution potential in the shallower water column there (**Figure 2**). This ^{224}Ra is then primarily dispersed laterally (that is, near the surface) due to $K_x >> K_z$ in the simulations.

The assessment of the effect of seabed slope (m) required a small modification to the finite difference model, where the thickness of the cells on the z-axis was modified (to 1 m for $m = 0.005$ and 4 m for $m = 0.02$). These simulations suggested that a bias associated with slow vertical mixing would tend to become more significant along transects with deeper mixed layers (**Figures 5G–I**), especially farther offshore.

DISCUSSION

Whilst the simulations were based on a simplistic representation of solute transport in coastal environments, especially for vertical mixing (Pacanowski and Philander, 1981; Durski et al., 2004), they clearly indicated that short-lived radiotracers like ^{223}Ra and ^{224}Ra may have a non-uniform vertical activity distribution

in shelf environments when vertical dispersion is low. This is of concern for the design of sampling programs for SGD tracers in coastal environments, where only surface water samples are often collected. Moreover, it is not possible to generalize if there will be a tendency to under- or overestimate whole water column activities by surface water sampling because this will be in part determined by other factors, such as location along the transect, K_x, and the source and magnitude of the tracer flux.

TABLE 1 | Literature estimates for K_z in different marine environments.

K_z (m^2 s^{-1})	Location	References
7.5×10^{-6}	Monterey Bay Shelf, California	Moniz et al., 2014
9×10^{-5}	Swan River Estuary, Australia	Etemad-Shahidi and Imberger, 2001
5×10^{-5} to 1.5×10^{-4}	Southwest Gulf of Maine	Benitez-Nelson et al., 2000
2.7×10^{-4}	North West Shelf, Australia	Webster, 1986
4×10^{-4}	Sea of Japan	Okubo, 1980
2×10^{-3}	Inner Shelf, Bering Sea	Glover and Reeburgh, 1987
10^{-3} to 10^{-2}	Southern Ocean	Charette et al., 2007
10^{-4} to 10^{-3}	Atlantic Ocean	Broecker et al., 1967
10^{-2}	Pacific Ocean	Broecker et al., 1967
10^{-6} to 10^{-1}	Indonesian Archipelago	Koch-Larrouy et al., 2015
10^{-2}	Surf zone	Kumar and Feddersen, 2017

Whilst methodology vary, the lower K_z are typically associated with coastal environments rather than the open ocean.

TABLE 2 | Parameter range for K_z, K_x, F_o, and F_B used in the simulations.

Variable	Range	References
K_z (m^2 s^{-1})	10^{-6}, $\underline{10^{-5}}$, 10^{-4}, 10^{-3}, and 10^{-2}	Refer to **Table 1**
K_x (m^2 s^{-1})	0.01, 0.1, $\underline{1}$, 10, and 100	de Silva Samarasinghe et al., 2003; Colbert and Hammond, 2007; Lamontagne and Webster, 2019
F_o and F_B (Bq m^{-1} s^{-1})		
^{223}Ra and ^{224}Ra	0.01, 0.1, $\underline{1}$, 10, 1, and 00	Lamontagne et al., 2015; Lamontagne and Webster, 2019
^{228}Ra	10^{-5}, 10^{-4}, $\underline{10^{-3}}$, and 10^{-2}	Lamontagne et al., 2015; Lamontagne and Webster, 2019
^{226}Ra	10–^{6}, 10^{-5}, $\underline{10^{-4}}$, and 10^{-3},	Lamontagne et al., 2015; Lamontagne and Webster, 2019
Seabed slope (*m*)	0.002, $\underline{0.01}$, and 0.02	

Underlined values represents the default unless otherwise noted in the text. For simplicity, a similar range in F_o and F_B was used for a given isotope to contrast the effect of the coastal and benthic Ra sources.

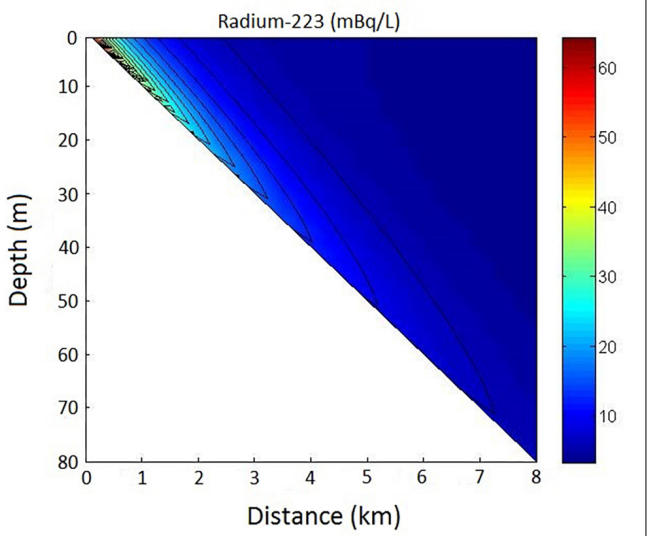

FIGURE 2 | Variations in ^{223}Ra activity in the water column for a relatively low K_z (10^{-6} m^2 s^{-1}) and high K_x (10 m^2 s^{-1}).

Lietzke and Lerman (1975) made similar observations to this study when evaluating the role of anisotropy in diffusivity on the vertical distribution in ^{222}Rn in Santa Barbara Basin. As for ^{223}Ra and ^{224}Ra distribution along a sloping seabed evaluated here, they found that much of the ^{222}Rn in the water column of this basin was from benthic production at shallower depth moving laterally owing to $K_x >> K_z$. The basin also had a noticeable vertical gradient in ^{222}Rn activity. Levy and Moore (1985) occasionally observed vertical ^{224}Ra gradients in the mixed layer off the coast of North Carolina and Georgia, which they attributed to a ^{224}Ra input from the seafloor. Such gradients may be more common than previously recognized for shelf environments.

Comparison With Characteristic Mixing Timescales

The simulation results are consistent with a qualitative assessment of the characteristic timescales of vertical mixing relative to radioactive decay. In general, transport processes tend to be less important in the mass-balance of a tracer when they occur more slowly than radioactive decay. For example, the characteristic timescale for vertical mixing by dispersion will be L^2/K_z, where L (m) is a representative mixed layer thickness. If $L^2/K_z >> 1/\lambda$, then vertical mixing is unlikely to contribute to differences in Ra activity in the water column. For example, assuming L = 20 m and $K_z = 10^{-5}$ m^2 s^{-1}, the characteristic timescale for vertical mixing will be 4×10^7 s, whereas the timescales for radioactive decay (=$1/\lambda$) are 4.6×10^5 s, 1.4×10^6 s, 2.6×10^8 s, and 7.2×10^{10} s for ^{224}Ra, ^{223}Ra, ^{228}Ra, and ^{226}Ra, respectively. This scaling is consistent with the numerical simulations performed here, which showed large vertical variations in activity due to slow mixing for ^{224}Ra and ^{223}Ra, small variations for ^{228}Ra, and no effect for ^{226}Ra.

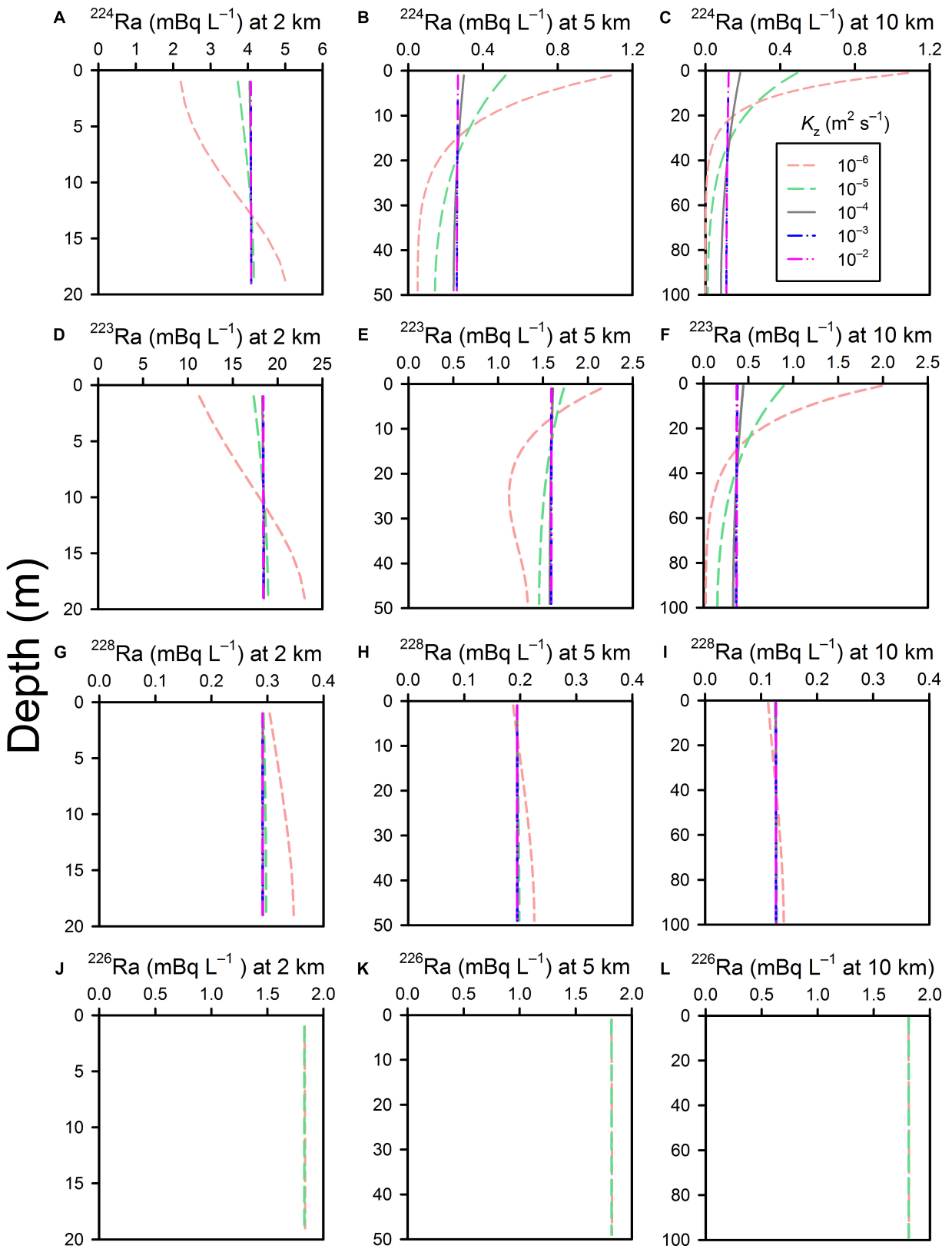

FIGURE 3 | Vertical variations in Ra activity for a range in K_z values for ^{223}Ra **(A–C)**, ^{224}Ra **(D–F)**, ^{228}Ra **(G–I)**, and ^{226}Ra **(J–L)** at 2 km (left column), 5 km (middle column) and 10 km from the coastline (right column).

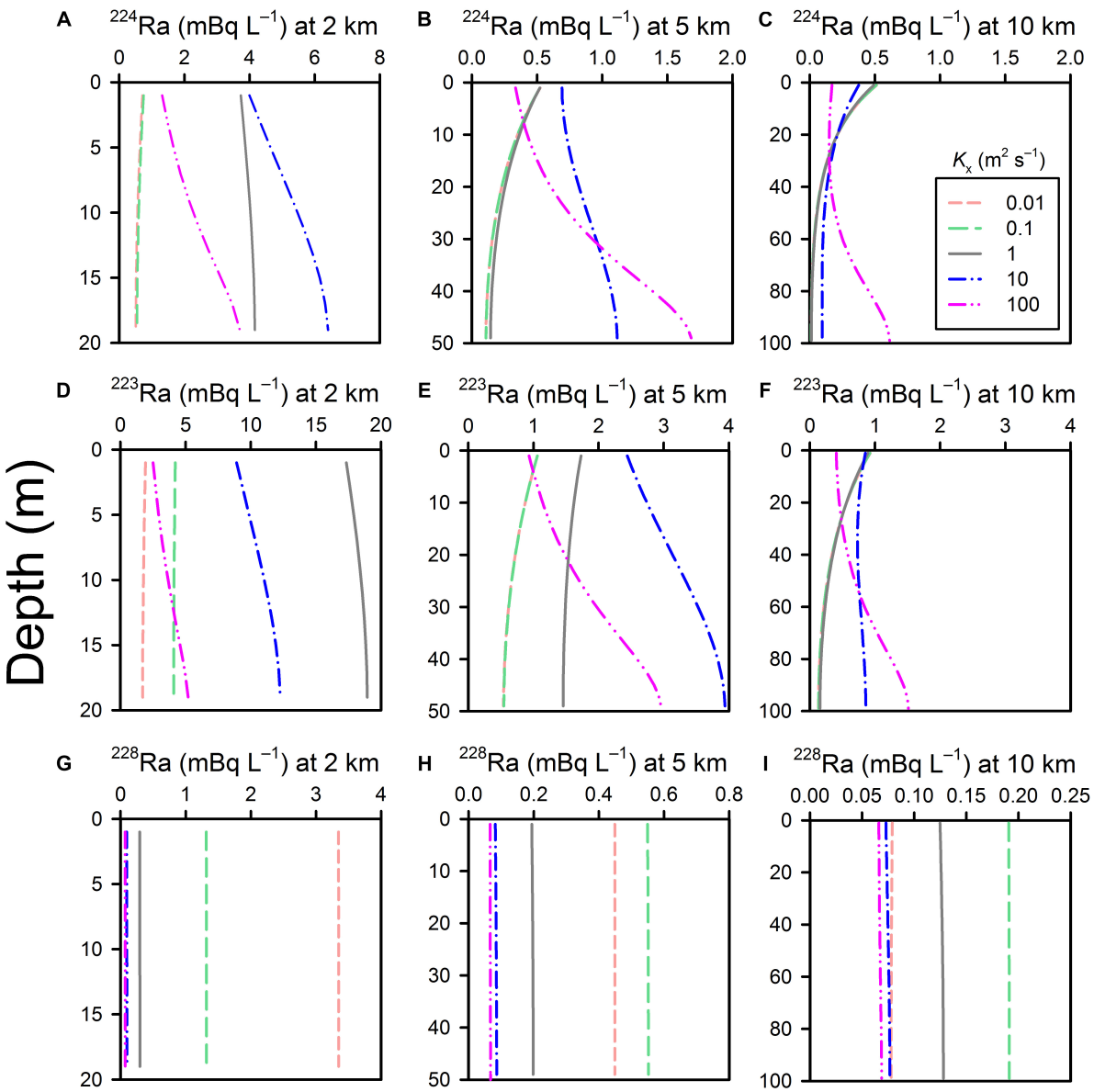

FIGURE 4 | Variations in ^{224}Ra **(A–C)**, ^{223}Ra **(D–F)**, and ^{228}Ra **(G–I)** activity as a function of K_x for a relatively low K_z value (10^{-5} m^2 s^{-1}) at 2 km (left column), 5 km (middle column), and 10 km (right column).

Radon-222 is another common SGD tracer (Stieglitz et al., 2013; Tait et al., 2016) with a half-life (3.82 days) comparable to ^{224}Ra. Thus, surface water sampling for ^{222}Rn may similarly, not be representative of the whole water column activity when the vertical mixing rate is low. Being a dissolved gas, a further complication with ^{222}Rn would be degassing, which has a characteristic timescale L/v (where v is the degassing velocity). The characteristic degassing timescale for ^{222}Rn would typically be slightly slower than its timescale for radioactive decay. For example, for L = 20 m and v = 1 m day^{-1} ($\sim$1.2 $\times$ 10^{-5} m s^{-1}), the characteristic timescale for degassing is $\sim$2 $\times$ 10^6 s (relative to $\sim$5 $\times$ 10^5 s for radioactive decay). This is also similar to the timescale of vertical mixing 4 $\times$ 10^6 s for $\sim K_z$ = 10^{-4} m^2 s^{-1} and L = 20 m. Thus, slow vertical mixing may impact on ^{222}Rn activities in the water column because it can be slower than the timescales of both radioactive decay and degassing.

K_z

A potentially mitigating or complicating factor in our analysis is that a constant K_z was assumed across the model domain, which may be unrealistic in some field settings (Koch-Larrouy et al., 2015). K_z is an empirical parameter summing-up a range of potential dispersive

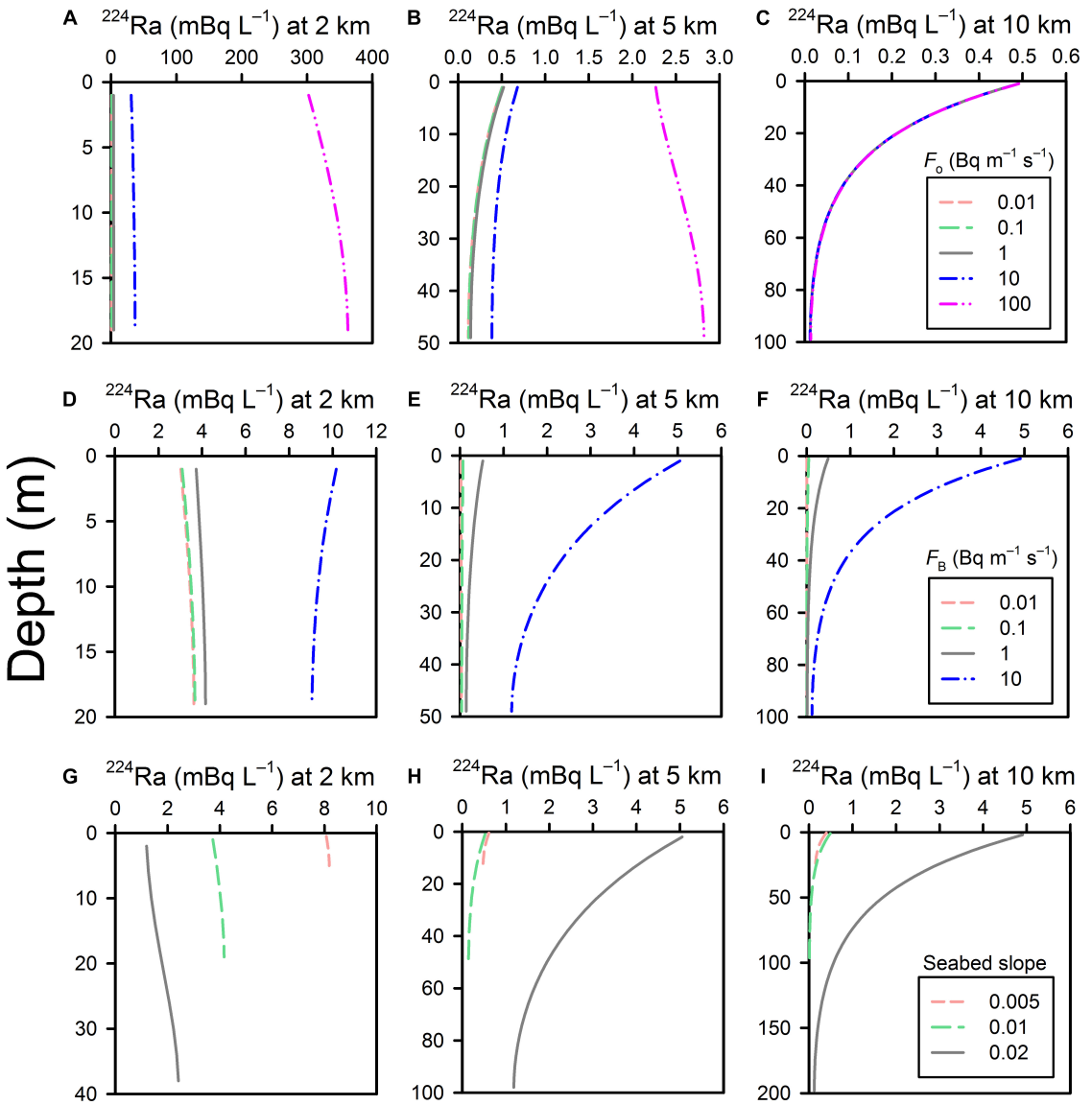

FIGURE 5 | Effects of variations in F_o **(A–C)**, F_B **(D–F)**, and seabed slope **(G–I)** on the vertical distribution of ^{224}Ra for a relatively low K_z value (10^{-5} m^2 s^{-1}).

processes induced by wind, tides, and other driving forces. As per other similar empirical dispersion parameters, K_z should be anticipated to be scale-, and time-dependent. For example, K_z can change significantly between calm and stormy conditions (Manucharyan et al., 2011) or following changes in wind direction (Kirincich and Barth, 2009). Some coastal embayments have periods with no tidal movements (de Silva Samarasinghe, 1998), which should also temporarily reduce K_z. This temporal variations in K_z could either mitigate or accentuate biases arising from surface sampling for tracers. As an example, if atmospheric fronts generating greater K_z have a characteristic timescale less then radioactive decay for a given tracer, the increased mixing of the water column they generate would tend to homogenize water column activities. Considering the paucity of data about vertical variations in Ra activity in inner shelf environments, the simple representation of K_z used here is probably sufficient on a preliminary basis.

Quantifying the Bias

Due to the paucity of information on vertical variability in Ra activity for inner shelves, it is not possible here to test the findings of this theoretical assessment with measurements under different field conditions. The potential magnitude of the bias can be evaluated here by comparing the longitudinal profiles for Ra from surface water relative to the depth-averaged values across the mixed layer generated from the simulations. For simplicity, this evaluation will be restricted to ^{224}Ra (a worse-case scenario due to its short half-life). The evaluation will be made for K_z varying from 10^{-6} to 10^{-4} m^2

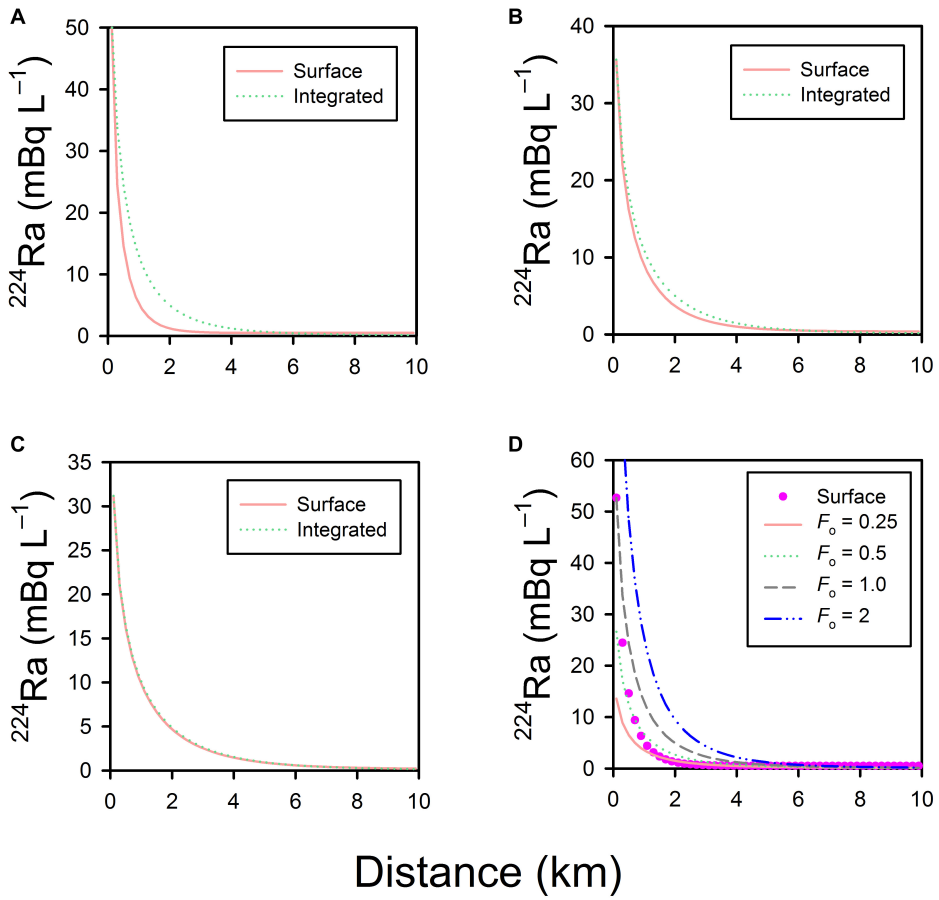

FIGURE 6 | Comparison of longitudinal Ra profile between surface samples and depth-averaged ^{224}Ra activities for **(A)** $K_z = 10^{-6}$ m^2 s^{-1}, **(B)** $K_z = 10^{-5}$ m^2 s^{-1}, and **(C)** $K_z = 10^{-4}$ m^2 s^{-1} (for $K_x = 10$ m^2 s^{-1}, F_o, and $F_B = 1$ Bq m^{-1} s^{-1}). **(D)** Evaluation of the bias in F_o when only using surface relative to depth-average ^{224}Ra activities.

s^{-1} (and for $K_x = 10$ m^2 s^{-1}, $F_o = 1$ Bq m^{-1} s^{-1} and $F_B = 1$ Bq m^{-1} s^{-1}).

Consistent with previous analyses, the bias was greatest for $K_z = 10^{-6}$ m^2 s^{-1} between surface and depth-average ^{224}Ra activities, with a tendency for surface samples to underestimate activities inshore and slightly overestimate activities offshore (**Figure 6A**). The bias was less pronounced for $K_z = 10^{-5}$ m^2 s^{-1} and negligible for $K_z = 10^{-4}$ m^2 s^{-1} (**Figures 6B,C**). For $K_z = 10^{-6}$ m^2 s^{-1}, simulations were then run to better match the "observed" surface ^{224}Ra activities using different F_o values (with K_x and F_B remaining unchanged). The closest match to the surface ^{224}Ra activities was for $F_o \sim 0.25$ to 0.50 Bq m^{-2} s^{-1}, or 50–75% of the correct value (1 Bq m^{-1} s^{-1}) (**Figure 6D**). Whilst only a crude evaluation in the absence of field measurements, this analysis suggests the bias caused by surface water sampling when K_z is low could be important.

CONCLUSION

There is a paucity of vertical Ra profiles over inner continental shelves. We demonstrated here that when vertical mixing is slow, vertical variations in short-lived radionuclides activity in a coastal mixed layer are possible. This is of concern for field programs aiming to measure SGD or other processes using these tracers. When the water column is not well mixed relative to a given tracer, only sampling near the surface (the current practice) will lead to biased estimates of the spatial distribution of the tracer and, consequently, of the inferred SGD estimates. Despite the significant effort required to collect Ra samples from seawater (Henderson et al., 2013), future field programs for SGD tracers over continental shelves should aim to collect at least one vertical profile in the mixed layer for short-lived tracers to evaluate the potential for slow vertical mixing. A potential benefit in measuring the vertical distribution in SGD tracers in the water column could be to help evaluate its recirculated component, which has a large component originating from the seabed.

DATA AVAILABILITY

No new dataset was generated in this study. The MATLAB script used to perform the simulations is available as **Supplementary Material**.

AUTHOR CONTRIBUTIONS

SL scoped the theoretical analysis, did the numerical simulations, and drafted the manuscript. IW contributed to the theoretical development and drafting of the manuscript.

FUNDING

This manuscript was made possible by funding from CSIRO Land & Water to SL.

ACKNOWLEDGMENTS

We acknowledge the insightful comments from reviewers on a previous publication, who recommended that we also explore biases associated with vertical dispersivity.

SUPPLEMENTARY MATERIAL

The Supplementary Material for this article can be found online at: https://www.frontiersin.org/articles/10.3389/fmars.2019.00357/full#supplementary-material

REFERENCES

Benitez-Nelson, C. R., Buesseler, K. O., and Crossin, G. (2000). Upper ocean carbon export, horizontal transport, and vertical eddy diffusivity in the southwestern gulf of Maine. *Cont. Shelf Res.* 20, 707–736. doi: 10.1016/s0278-4343(99)00093-x

Broecker, W. S., Li, Y. H., and Cromwell, J. (1967). Radium-226 and radon-222: concentration in atlantic and pacific oceans. *Science* 158, 1307–1310. doi: 10.1126/science.158.3806.1307

Burnett, W. C., Bokuniewicz, H., Huettel, M., Moore, W. S., and Taniguchi, M. (2003). Groundwater and pore water inputs to the coastal zone. *Biogeochemistry* 66, 3–33. doi: 10.1023/b:biog.0000006066.21240.53

Charette, M. A., Gonneea, M. E., Morris, P. J., Statham, P., Fones, G., Planquette, H., et al. (2007). Radium isotopes as tracers of iron sources fueling a southern ocean phytoplankton bloom. *Deep Sea Res. Part 2 Top. Stud. Oceanogr.* 54, 1989–1998. doi: 10.1016/j.dsr2.2007.06.003

Charette, M. A., and Scholten, J. C. (2008). Marine chemistry special issue: the renaissance of radium isotopic tracers in marine processes studies. *Mar. Chem.* 109, 185–187. doi: 10.1016/j.marchem.2008.04.001

Chung, Y.-C., and Craig, H. (1973). Radium-226 in the eastern equatorial pacific. *Earth Planet. Sci. Lett.* 30, 306–318. doi: 10.1016/0012-821x(73)90195-7

Colbert, S. L., and Hammond, D. E. (2007). Temporal and spatial variability of radium in the coastal ocean and its impact on computation of nearshore cross-shelf mixing rates. *Cont. Shelf Res.* 27, 1477–1500. doi: 10.1016/j.csr.2007.01.003

de Silva Samarasinghe, J. R. (1998). Revisiting upper gulf st vincent in south australia: the salt balnace and its implications. *Estuar. Coast Shelf Sci.* 46, 51–63. doi: 10.1006/ecss.1997.0249

de Silva Samarasinghe, J. R., Bode, L., and Mason, L. B. (2003). Modelled response of gulf st vincent (South Australia) to evaporation, heating and winds. *Cont. Shelf Res.* 23, 1285–1313. doi: 10.1016/s0278-4343(03)00129-8

Dulaiova, H., and Burnett, W. C. (2006). Radon loss across the water-air interface (Gulf of Thailand) estimated experimentally from222Rn-224Ra. *Geophys. Res. Lett.* 33:L05606.

Durski, S. M., Glenn, S. M., and Haidvogel, D. B. (2004). Vertical mixing schemes in the coastal ocean: comparison of the level 2.5 mellor-yamada scheme with an enhanced version of the K profile parameterazation. *J. Geophys. Res.* 109:C01015.

Etemad-Shahidi, A., and Imberger, J. (2001). The estimation of vertical eddy diffusivity in estuaries. *Water Pollut.* 3, 455–463.

Glover, D. M., and Reeburgh, W. S. (1987). Radon-222 and radium-226 in southeastern bering sea shelf waters and sediments. *Cont. Shelf Res.* 7, 433–456. doi: 10.1016/0278-4343(87)90090-2

Hancock, G. J., Webster, I. T., and Stieglitz, T. C. (2006). Horizontal mixing of great barrier reef waters: offshore diffusivity determined from radium isotope distribution. *J. Geophys. Res. Oceans* 111:C12019.

Henderson, P. B., Morris, P. J., Moore, W. S., and Charette, M. A. (2013). Methodological advances for measuring low-level radium isotopes in seawater. *J. Radioanal. Nucl. Chem.* 296, 357–362. doi: 10.1007/s10967-012-2047-9

Kirincich, A. R., and Barth, J. A. (2009). Time-Varying across-shelf ekman transport and vertical eddy viscosity on the inner shelf. *J. Phys. Oceanogr.* 39, 602–620. doi: 10.1175/2008jpo3969.1

Knee, K. L., Garcia-Solsona, E., Garcia-Orellana, J., Boehm, A. B., and Paytan, A. (2011). Using radium isotopes to characterize water ages and coastal mixing rates: a sensitivity analysis. *Limnol. Oceanogr. Methods* 9, 380–395. doi: 10.4319/lom.2011.9.380

Koch-Larrouy, A., Atmadipoera, A., Van Beek, P., Madec, G., Aucan, J., Lyard, F., et al. (2015). Estimates of tidal mixing in the indonesian archipelago from multidisciplinary INDOMIX in-situ data. *Deep Sea Res. Part 1 Oceanogr. Res. Pap.* 106, 136–153. doi: 10.1016/j.dsr.2015.09.007

Kumar, N., and Feddersen, F. (2017). The effect of stokes drift and transient rip currents on the inner shelf. part I: no stratification. *J. Phys. Oceanogr.* 47, 227–241. doi: 10.1175/jpo-d-16-0076.1

Lamontagne, S., La Salle, C. L., Hancock, G. J., Webster, I. T., Simmons, C. T., Love, A. J., et al. (2008). Radium and radon radioisotopes in regional groundwater, intertidal groundwater, and seawater in the adelaide coastal waters study area: implications for the evaluation of submarine groundwater discharge. *Mar. Chem.* 109, 318–336. doi: 10.1016/j.marchem.2007.08.010

Lamontagne, S., Taylor, A. R., Herpich, D., and Hancock, G. J. (2015). Submarine groundwater discharge from the South Australian limestone coast region estimated using radium and salinity. *J. Environ. Radioact.* 140, 30–41. doi: 10.1016/j.jenvrad.2014.10.013

Lamontagne, S., and Webster, I. T. (2019). Cross-Shelf transport of submarine groundwater discharge tracers: a sensitivity analysis. *J. Geophys. Res. Oceans* 124, 453–469. doi: 10.1029/2018jc014473

Levy, D. M., and Moore, W. S. (1985). 224Ra in continental shelf waters. *Earth Planet. Sci. Lett.* 73, 226–230. doi: 10.1016/0012-821x(85)90071-8

Li, C. Y., and Cai, W. J. (2011). On the calculation of eddy diffusivity in the shelf water from radium isotopes: high sensitivity to advection. *J. Mar. Syst.* 86, 28–33. doi: 10.1016/j.jmarsys.2011.01.003

Lietzke, T. A., and Lerman, A. (1975). Effects of bottom relief in two-dimensional oceanic eddy diffusion models. *Earth Planet. Sci. Lett.* 24, 337–344. doi: 10.1016/0012-821x(75)90139-9

Manucharyan, G. E., Brierley, C. M., and Fedorov, A. V. (2011). Climate impacts of intermittent upper ocean mixing induced by tropical cyclones. *J. Geophys. Res. Oceans* 116:C11038.

Moniz, R. J., Fong, D. A., Woodson, C. B., Willis, S. K., Stacey, M. T., and Monismith, S. G. (2014). Scale-dependent dispersion within the stratified interior on the shelf of northern monterey bay. *J. Phys. Oceanogr.* 44, 1049–1064. doi: 10.1175/jpo-d-12-0229.1

Moore, W. S. (2000). Determining coastal mixing rates using radium isotopes. *Cont. Shelf Res.* 20, 1993–2007. doi: 10.1016/s0278-4343(00)00054-6

Moore, W. S. (2007). Seasonal distribution and flux of radium isotopes on the southeastern U.S. continental shelf. *J. Geophys. Res.* 112:C10013. doi: 10.1016/s0278-4343(00)00054-6

Moore, W. S. (2015). Inappropriate attempts to use distributions of 228Ra and 226Ra in coastal waters to model mixing and advection rates. *Cont. Shelf Res.*105, 95–100. doi: 10.1016/j.csr.2015.05.014

Moore, W. S., Astwood, H., and Lindstrom, C. (1995). Radium isotopes in coastal waters on the Amazon shelf. *Geochim. Cosmochim. Acta* 59, 4285–4298. doi: 10.1016/0016-7037(95)00242-r

Okubo, T. (1980). Radium-228. *J. Oceanogr. Soc. Japan* 36, 263–268.

Pacanowski, R. C., and Philander, S. G. H. (1981). Parameterizationof vertical mixing in numerical moels of tropical oceans. *J. Phys. Oceanogr.* 11, 1443–1451. doi: 10.1175/1520-0485(1981)011<1443:povmin>2.0.co;2

Stieglitz, T. C., Clark, J. F., and Hancock, G. J. (2013). The mangrove pump: the tidal flushing of animal burrows in a tropical mangrove forest determined from radionuclide budgets. *Geochim. Cosmochim. Acta* 102, 12–22. doi: 10.1016/j.gca.2012.10.033

Tait, D. R., Maher, D. T., Macklin, P. A., and Santos, I. R. (2016). Mangrove pore water exchange across a latitudinal gradient. *Geophys. Res. Lett.* 43, 3334–3341. doi: 10.1002/2016gl068289

Webster, I. T. (1986). The vertical structure of currents on the north west shelf of australia at subtidal frequencies. *J. Phys. Oceanogr.* 16, 1145–1157. doi: 10.1175/1520-0485(1986)016<1145:tvsoco>2.0.co;2

Conflict of Interest Statement: The authors declare that the research was conducted in the absence of any commercial or financial relationships that could be construed as a potential conflict of interest.